Acta Materialia 219 (2021) 117225

Contents lists available at ScienceDirect

Acta Materialia

journal homepage: www.elsevier.com/locate/actamat

Full length article

Deformation twin interactions with grain boundary particles in multi-phase magnesium alloys

B. Anthony[a,*], B. Leu[b], I.J. Beyerlein[b], V.M. Miller[a]

[a] Department of Materials Science and Engineering, University of Florida, Gainesville, Florida, 32611, USA
[b] Department of Materials Science and Engineering, University of California Santa Barbara, Santa Barbara, California, USA

ARTICLE INFO

Article history:
Received 15 January 2021
Revised 29 July 2021
Accepted 30 July 2021
Available online 11 August 2021

Keywords:
Magnesium alloys
Deformation twinning
Twin transmission
Intermetallic phases

ABSTRACT

Deformation twinning is necessary for achieving strain in plastically hard directions in magnesium alloys under ambient conditions, but can also contribute to void formation and crack propagation that lead to early failure. This is especially true for instances of twin transmission between grains, which result in longer continuous twin boundaries and higher twin volume fractions. Coarse grain boundary particles have the potential to modify twinning behavior, but this effect has not been studied. This work uses a Crystal Plasticity – Fast Fourier Transform model to predict twinning behavior and transmission likelihood, parameterized to simulate different morphologies of the β-phase intermetallic common to Mg-Al alloys. Of these microstructures, those with particles directly in the path of impingement were found to decrease the stresses generated in the neighboring grain, similarly decreasing the likelihood of twin transmission across the boundary. Size and aspect ratio were found to play key roles in determining the resultant stress, but are dependent upon the orientation of the neighboring grain. Particles located near the impingement site were found to exacerbate the stress state and make transmission more likely. Instances where transmission was likely to be prevented were also predicted to undergo reduced twin thickening.

1. Introduction

Controlling deformation twinning via microstructural engineering has been a long-employed strategy for reducing the undesirable plastic anisotropy in Mg alloys [1]. However, the studies to date have largely focused on single-phase alloys, while many commercial alloys have a substantial volume fraction of intermetallic particles [1–3]. When two-phase alloys are considered, focus is usually placed on nano-scale precipitates rather than micron-sized primary particles [4,5]. This work investigates how deformation twinning interacts with grain boundary particles found in as-solidified commercial alloys to enable more thorough microstructural control.

While a certain degree of twinning aids in arbitrary deformation of a bulk material, further twinning can lead to premature failure [6]. Since twins have a distinct orientation relationship to their parent grain, profuse twin formation and growth can rapidly modify a pre-existing texture [7]. This change in orientation also affects the Schmid factors for slip within the twinned region, making particular slip systems relatively easier or harder than in the parent grain [8]. The $\{10\bar{1}1\}$-$\{10\bar{1}2\}$ double twins have been shown to serve as void nucleation sites that can initiate cracking [6]. These cracks can then propagate along the $\{10\bar{1}2\}$ tension twin interfaces, which provide a favorable fracture pathway which ultimately aids failure [9]. The twin fraction has been shown to be independent of grain size, although larger grains tend to have more twins per grain [10,11].

Easy crack propagation paths are often formed by twin chains, which result from twin transmission across grain boundaries [12]. When the tip of a twin propagates across its parent grain and reaches the grain boundary, a local shear is imposed in the boundary [13]. The intense local shear imposed on the neighboring grain and the ability of the boundary to act as a source of twinning dislocations combine to promote nucleation of a new twin in the neighboring grain. Twin transmission has been both experimentally and computationally shown to occur more readily between grains of lower misorientation [10,14]. In a highly textured material, which is inherently more likely to have many low misorientation boundaries, twin chains are likely to form and serve as potential crack pathways [15]. Twin transmission events have also been shown to affect the twin variant that nucleates in the neighboring grain, reportedly causing non-Schmid variant selection in the secondary twins [10].

* Corresponding author.
E-mail address: benjamin.anthony@ufl.edu (B. Anthony).

https://doi.org/10.1016/j.actamat.2021.117225

The likelihood of twin growth—the thickening of twins—also increases the overall twin volume fraction. Once a twin has nucleated across a grain and reached the opposing boundary, the constraint of the neighboring grains on the sheared parent generates a backstress that prevents the outward expansion of the twin interfaces [13,16]. The twinning resolved shear stress (TRSS)—that is, the resolved shear stress in the twinning plane and direction—must locally increase again before the twinning dislocations at the interfaces can move, thereby thickening the twinned region [17]. Since these backstresses tend to be less severe further away from the grain boundaries, growth tends to occur more readily in the center of the twin, leading to the familiar lenticular shape. Twin growth is affected by the elastic properties of the material, with more elastically isotropic materials such as Mg growing thicker twins than those that are more anisotropic, such as Zr [18]. Lower misorientation angles between the parent grain and its neighbors result in a decrease in the generated backstresses that also leads to thicker twins [10]. In instances of twin transmission, the adjoining twin pairs are observed to grow thicker than independent twins, owing to an even greater decrease in backstresses [10,19].

To date, computational studies on twin transmission and growth in magnesium and its alloys have focused on the interactions with just the grain boundary [13,14,16,18–21]. However, many commercial Mg alloys, particularly Al-rich alloys, feature coarse intermetallic particles in the as-solidified state of cast or thixomolded products [22–25]. Alloys such as AM60 form the β-$Mg_{17}Al_{12}$ phase as micron-scale particles along the boundaries. This β phase is elastically harder than the α-Mg matrix, [26,27] and at room temperature the β phase is brittle and experiences fracture instead of plastically deforming [28]. These β phase grain boundary particles have been shown to promote dynamic recrystallization and weaken deformation texture [29,30], as well as improve strength without reducing ductility, as even once the particles fracture the cracks are not observed to propagate into the matrix [3]. The presence of these hard particles at the grain boundary will necessarily alter the stress states generated in their vicinity due to mechanical mismatch, but prior studies have not considered the impact of this modification on twin growth or transmission.

The present study investigates the role these grain boundary particles play on twin transmission and growth behavior. The effects of particle properties, size, shape, and location relative to the twin tip are considered, along with the effects of the neighbor grain orientation. The likelihood of twin transmission, the backstresses in the parent grain, and the relative twin thickening behavior is considered for each case.

2. Methodology

A Crystal Plasticity – Fast Fourier Transform modeling method was used to investigate the effects of intermetallic particles at the grain boundary on twin transmission. This technique allows for a spatially resolved examination of the stress fields that develop during straining. This particular CP-FFT model has been previously modified by Kumar et al. to account for the shear transformation that occurs due to twinning [13], allowing for detailed study of the effects of twins on the local stress states in the microstructure.

The general microstructure for the cases studied is set up as shown in Fig. 1. A bi-crystal structure is created, in which the primary (parent) grain orientation is held constant across all cases. The orientation of the secondary grain can be varied between cases, and is the area of interest for examining the stress states imposed by the twin tip across the grain boundary. The overall size of the simulation is $3 \times 500 \times 500$ voxels, with a 25 voxel wide buffer layer representing a randomly oriented polycrystal around the outer edge to account for the average bulk material response.

Table 1
Elastic tensor parameters (in GPa) and CRSS values (in MPa) used for the matrix and particle phases [26,27]. Note that β-$Mg_{17}Al_{12}$ is BCC and is parameterized to have no active slip systems.

Phase	C_{11}	C_{12}	C_{13}	C_{33}	C_{55}
α-Mg	59.75	23.24	21.70	61.70	16.39
β-$Mg_{17}Al_{12}$	88.38	23.54	-	-	26.95
β-$Mg_{17}Al_{12}$ (10× case)	883.8	235.4	-	-	269.5
Phase Basal	Prismatic	Pyramidal		T. Twin	
α-Mg 3.3	35.7	86.2		20.0	

Table 2
Orientation cases used in simulations, with Euler angles given in Bunge convention.

Case name	Euler angles of neighbor (degrees)	Misorientation angle (degrees)	Crystal frame
"Single Crystal"	0-0-0	0	
Basal Rotation	30-0-0	30	
Basal Tilt	0-30-0	30	
High Misorientation	50-43-30	47	

Periodic boundary conditions were used with the combined bicrystal and buffer layer serving as the periodic cell. The material is compressed in the Y-direction over 15 steps to generate the resolved shear stress necessary to initiate tension twinning, at which point a shear transformation corresponding to the $[01\bar{1}1](0\bar{1}12)$ variant is applied to the twin region within the parent grain until convergence is achieved (2000 steps) to determine the stresses that result from the twin shear. In all cases, the twin formed is 7 voxels wide for a twin volume of approximately 3%.

Material parameters are representative of a hypothetical Mg-Al alloy in which the bulk is pure magnesium with β-$Mg_{17}Al_{12}$ at the grain boundary. The matrix is parameterized with the elastic properties and CRSS values for pure Mg at room temperature [27]. Perfectly plastic slip behavior is assumed because of the small strains present in the simulations. Additionally, this assumption is consistent with related work in the literature [14,18], enabling direct comparisons. The β phase particle is elastically hard relative to the matrix, and is assumed to have no active slip systems at room temperature. The elastic properties for both phases and the CRSS values for the α matrix can be seen in Table 1 [26,27].

For modifying the orientation of the secondary grain, four discrete orientation cases were considered, as seen in Table 2. These specific orientations were selected from a list of orientations used by Kumar et al. as a way to discretely segment orientation space for similar studies, using only the cases below the 50° misorientation threshold for twin transmission in simulations [14,18]. The four orientations considered are the "single crystal" case (no misorientation), basal rotation, basal tilt, and a highly misoriented case close to the threshold.

Microstructural cases were selected to represent varying aspects of the particle morphology, properties, and location as seen in Fig. 2. The initial comparison cases are those of no particle being present and a circular particle (diameter, D = 50 voxels, ~ 7× twin thickness). The size of the particle relative to the twin thickness is considered with the small particle (D = 25 voxels, ~ 3.5× twin thickness) and large particle (D = 75 voxels, ~ 10.5× twin thickness) cases. The effects of the mechanical properties of the secondary phase are evaluated by taking the circular particle case and modifying the elastic properties to be 10 times their actual values. The location effects of the particle are investigated by shift-

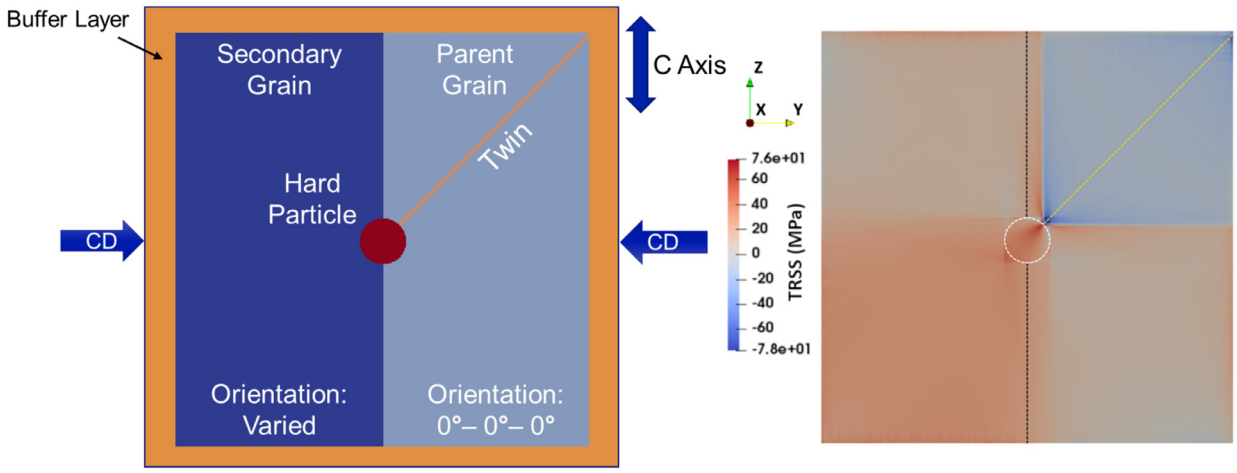

Fig. 1. Overview of the Crystal Plasticity – Fast Fourier Transform (CP-FFT) simulation, with resulting TRSS visualization for the parent twin variant.

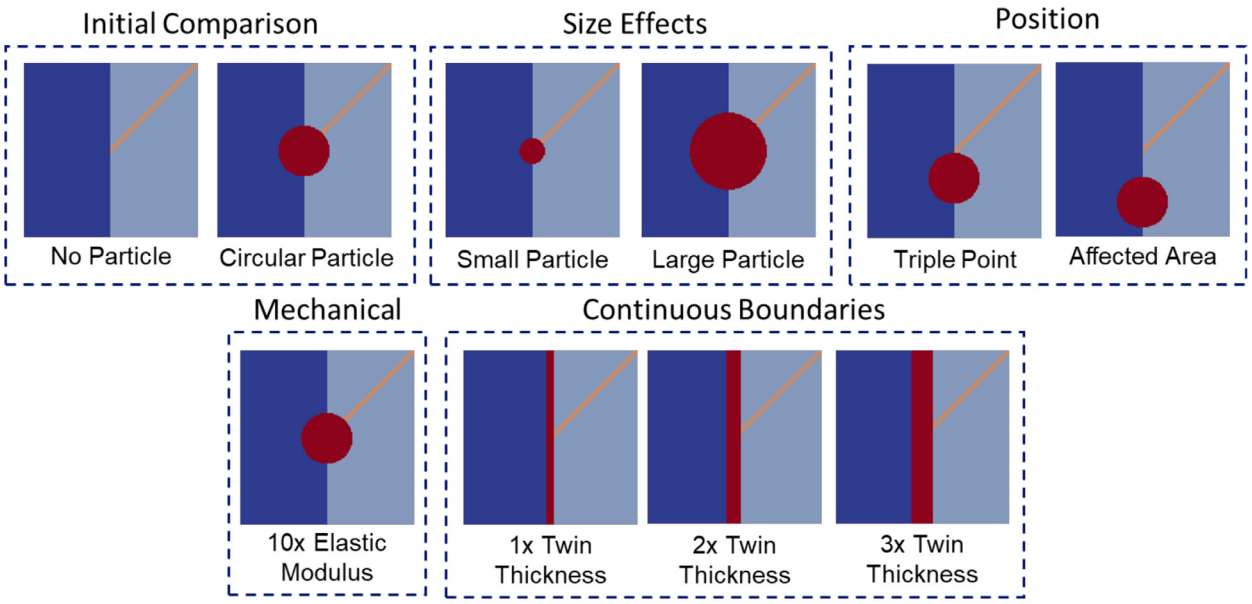

Fig. 2. Center regions of simulated microstructural cases considered for testing, modifying particle presence, morphology, properties, and location.

ing the circular particle down by 25 and 50 voxels, resulting in the twin tip impinging on the triple point and on the grain boundary within the stress-affected region of the secondary phase, respectively. Finally, the morphology of the β phase was changed by representing the precipitate as a continuous boundary rather than a discrete particle to mimic the as-solidified state of cast Mg-Al alloys [22,23]. In these cases, the thickness of the boundary is based off the thickness of the twin, resulting in continuous boundaries of 7 voxels, 14 voxels, and 21 voxels.

3. Results

3.1. Resolved shear stresses around twin tip

The stress tensors in a semi-circular region, designated Ω, of the secondary grain near the twin tip were considered, as seen in the inset in Fig. 3. While previous works using this method [14,20] have considered a fixed Ω region size, the varying presence, size, and location of the β-phase particle necessitates a different approach. In this work, the center of the Ω region is fixed and the radius of the Ω region was increased up to a maximum of 50 voxels to consider comparable areas across all particle shapes and sizes. The stress tensor at each voxel within this region (excluding those inside the particle) was resolved for each extension twin variant. These values were then averaged across the Ω region to find the mean TRSS of each twin variant within the secondary grain. The variant with the highest mean across the range of Ω radii was selected for comparison. Average TRSS was plotted against Ω region area as seen in Fig. 3. By changing the size of the Ω region and comparing with respect to equivalent areas, both short- and long-range effects on the stress states can be considered regardless of particle morphology.

Figure 3a and b compare the microstructural cases for the "single crystal" orientation where the grain pair has no misorientation. While the average TRSS with no particle is well above the threshold for twinning of 20 MPa, adding a particle of any size noticeably decreases the short-range stress within the secondary grain. This decrease is less apparent with a small particle which maintains a TRSS slightly above the CRSS for twinning, whereas the circular and large particle cases fall below the threshold. Instances of impingement near the particle at the triple point and in the affected area increase the TRSS above having no particle at all. For continuous boundaries, the TRSS only drops once the intermetallic layer is widened to more than 2× the twin thickness.

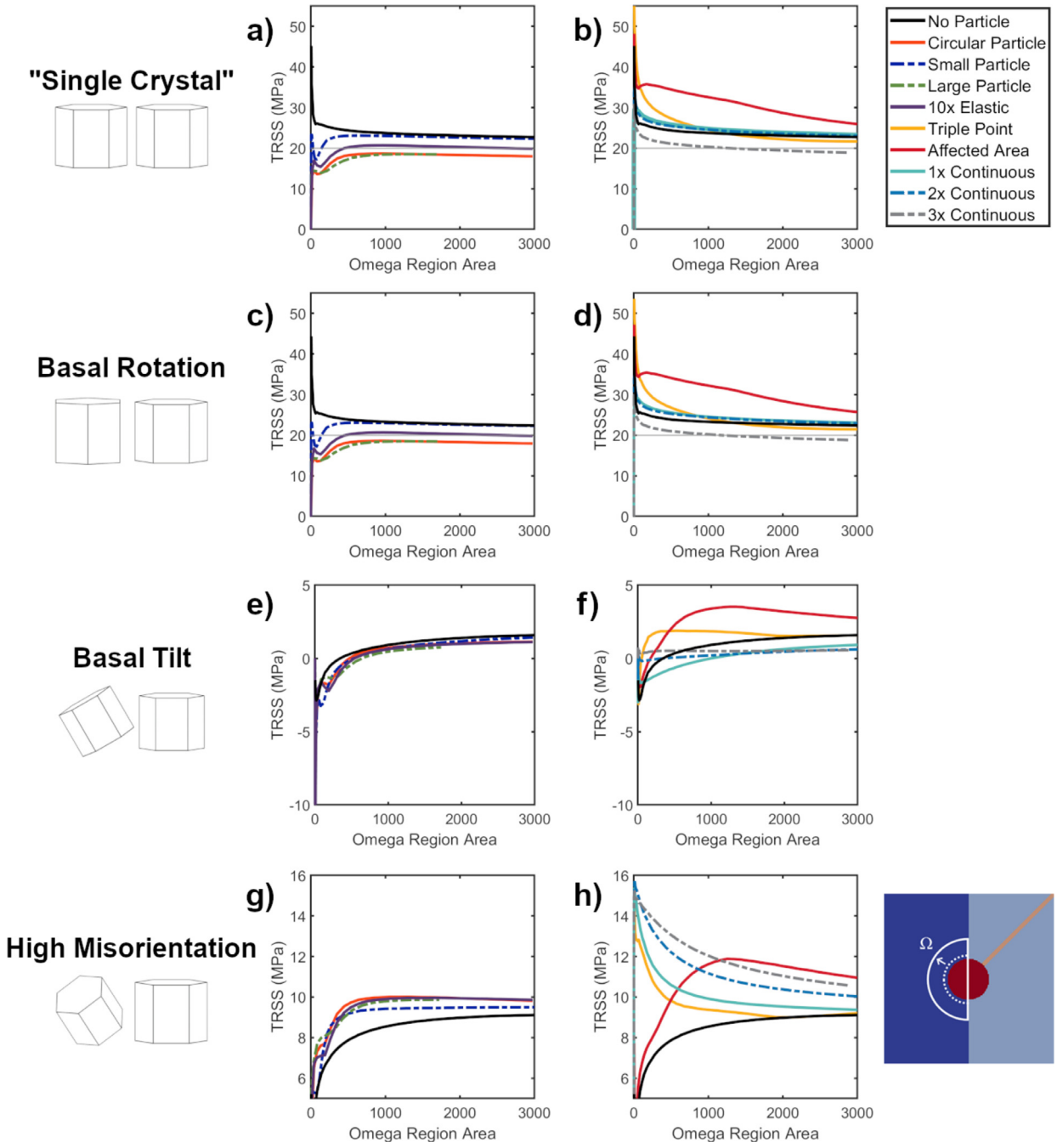

Fig. 3. Averaged twinning resolved shear stress values in the secondary grain within Ω regions of increasing area for the *a-b*) "single crystal", *c-d*) basal rotation, *e-f*) basal tilt, and *g-h*) high misorientation grain orientations. Microstructural cases are split between two plots with no particle (black) plotted for both to ease comparison. The CRSS for twinning used in the simulations (20 MPa) is shown in *a-d* in grey for comparison. Inset, bottom right: schematic of increasing Ω region size.

When the secondary grain is rotated around the *c*-axis, as seen in Fig. 3c and d, the TRSS values are almost identical to that of the "single crystal" orientation. Only minor variations are present between the two orientations, with the overall trends remaining the same. The particle leads to a reduction in the TRSS with respect to the no particle case, except when the twin skims the top of the particle at the triple junction or impinges nearby in the affected area.

Conversely, tilting the secondary grain on the *c*-axis, as seen in Fig. 3e and f, significantly decreases the TRSS values to well below the CRSS for twinning with the maximum within any Ω region being below 5 MPa. Unlike the other orientation cases, there are several instances of the average resolved shear stress being negative. Despite this, many of the same trends in the "single crystal" and basal rotation orientations are still present.

Figure 3g and h shows the highly misoriented grains, and results in contrast to the other orientations. In this orientation, the addition of any particle regardless of size, shape, location, or mechanical properties resulted in increased stresses over having no particle at all, albeit still below the CRSS for twinning. Additionally, as the Ω region grows, the small particle maintains a lower TRSS value than the circular and large particle. Unlike the other grain orientations, all three continuous boundary cases experience greater resolved stresses than having no particle at all, with thicker boundaries experiencing slightly higher stresses.

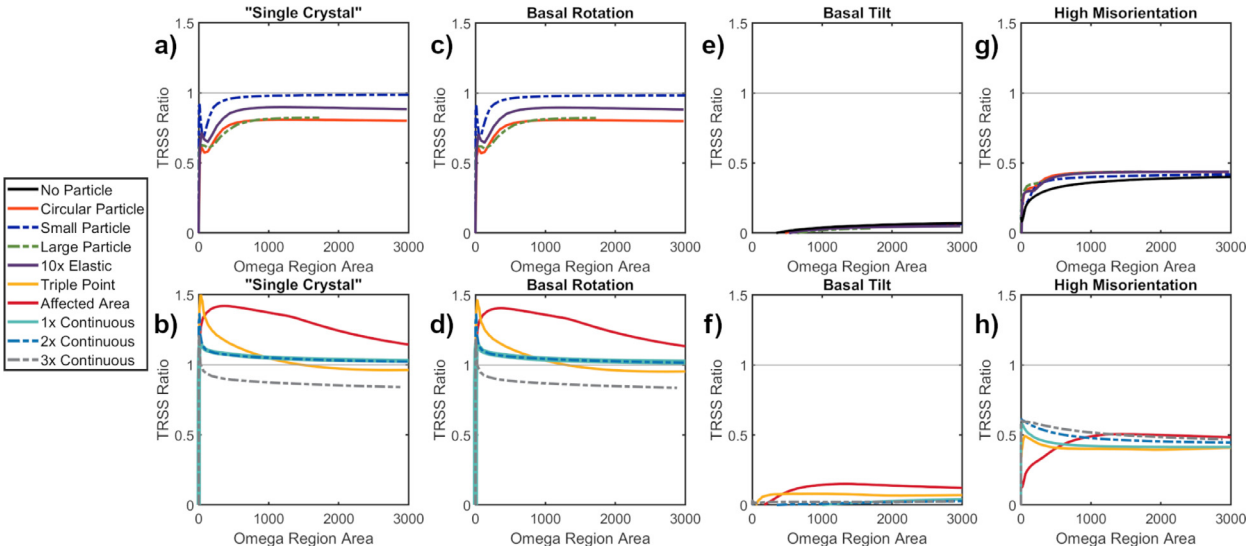

Fig. 4. Ratios of the TRSS values to twinning resolved shear stress in the "single crystal" case ($TRSS_{SX}$) across the range of microstructure and orientation cases, in which $TRSS_{SX}$ is the twinning resolved shear stress of the "single crystal" case with no particle, equivalent to propagation of the initial twin through its parent grain.

3.2. TRSS ratios

The likelihood of twin transmission can be made more apparent by normalizing the TRSS by the TRSS of the "single crystal" with no particle. These ratios can indicate that twin transmission has a high probability of occurring if the value is above 1, as this represents that the stresses are more favorable to nucleating a twin in the secondary grain than further twin propagation would be in a single crystal. Conversely, values below 1 represent a decreasing likelihood of twin transmission across the grain boundary. Values of 0 represent an instance where twin transmission is never expected.

Due to the similarity in the base values, the TRSS ratios for the "single crystal" case seen in Fig. 4a and b and the basal rotation case in Fig. 4c and d remain highly similar. The addition of a particle in the path of the twin decreases the TRSS ratio significantly at short range, then plateaus once the Ω region size is increased. While the circular particle and large particle cases are less likely to transmit even at this plateau, the small particle case reaches a ratio close to unity. The high modulus particle results in a similar trend to the circular particle, but shifted to a higher ratio plateau. Both the triple point and affected area cases have values well above that of the $TRSS_{SX}$ case near the impingement site, resulting in TRSS ratios well above 1 on the shorter end of the range that ultimately decrease with increasing Ω region size. The two thinner continuous boundaries were found to have nearly identical ratios that remain above unity across the entire range, whereas the thickest boundary (3× twin thickness) drops below unity.

In the instance of basal tilt seen in Fig. 4e and f, the overall values of the TRSS ratios are drastically decreased across all cases and ranges. While the triple point and affected area cases still maintain the trends observed in the previous two orientations of having values higher than the rest of the tested microstructures, these ratios still fall to a low likelihood of transmission, even at their peak. The highly misoriented grains in Fig. 4g and h similarly see an overall decrease from the "single crystal" orientation case, with most microstructures having a TRSS ratio at or below a value of 0.5. For both basal tilt and high misorientation, the particle effects on the stress state are largely washed out by the larger boundary misorientation effects.

3.3. Backstresses

The stress states in the CP-FFT simulations can also be used to determine the backstress generated within the parent grain by the twin, which is related to twin thickening. These stresses are found by taking the TRSS values for the parent twin variant along the center of the twin line before and after the twin transformation, as seen in Fig. 5a. The resulting difference in stress between the two is the backstress, and is usually lowest in the center of the grain. A central region within the parent grain of 50 voxels, denoted Σ in Fig. 5b, was taken at the beginning and end of the twinning transformation. The backstress was calculated for each point within Σ, then these values were averaged to compare the relative twin thickening behaviors for each case. Higher backstress within the parent grain result in less twin growth, ultimately leading to thinner twins.

The calculated backstresses for all microstructure and orientation cases can be seen in Fig. 6. While microstructure-dependent changes are apparent, the orientation between the parent and secondary grains has a more pronounced effect on modifying the expected twin thickening behavior. As in the previous sections, the "single crystal" and basal rotation orientation behave similarly. Compared to the case of no particle, the circular particle, large particle, increased elastic modulus, and the thickest continuous boundary cases all saw a significant increase in the generated backstress, indicating a propensity toward forming thinner twins. The small particle and two thinner boundary cases have stresses similar to that of the no particle case, indicating they have little impact on the original twin's thickening behavior. The triple point and affected area cases have a minor decrease, potentially leading to slightly thicker twins.

For the basal tilt and highly misoriented cases, many of the same trends are experienced as in the previous two orientations, although the impact of the microstructure on the backstress are diminished even in the most pronounced cases. However, a few minor deviations are noted. For both orientations, the small particle case is seen to have a greater backstress compared to no particle being present. Increasing the elastic modulus for the particle in the highly misoriented grain orientation results in a backstress approximately equal to that of the case with no particle be-

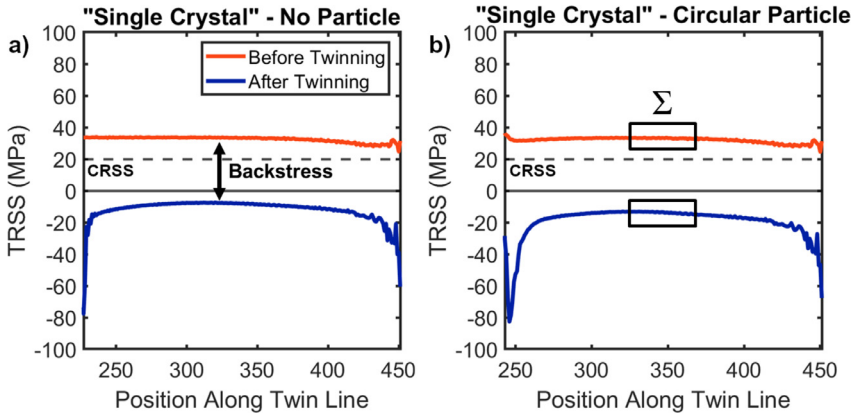

Fig. 5. Method of determining backstress within a grain using the TRSS values for the parent twin variant. *a*) TRSS before and after twinning across the one-dimensional line of the of the initial twin in the "single crystal" orientation case with no particle, with backstress shown. *b*) TRSS before and after twinning in the circular particle case, "single crystal" orientation with center Σ region designated.

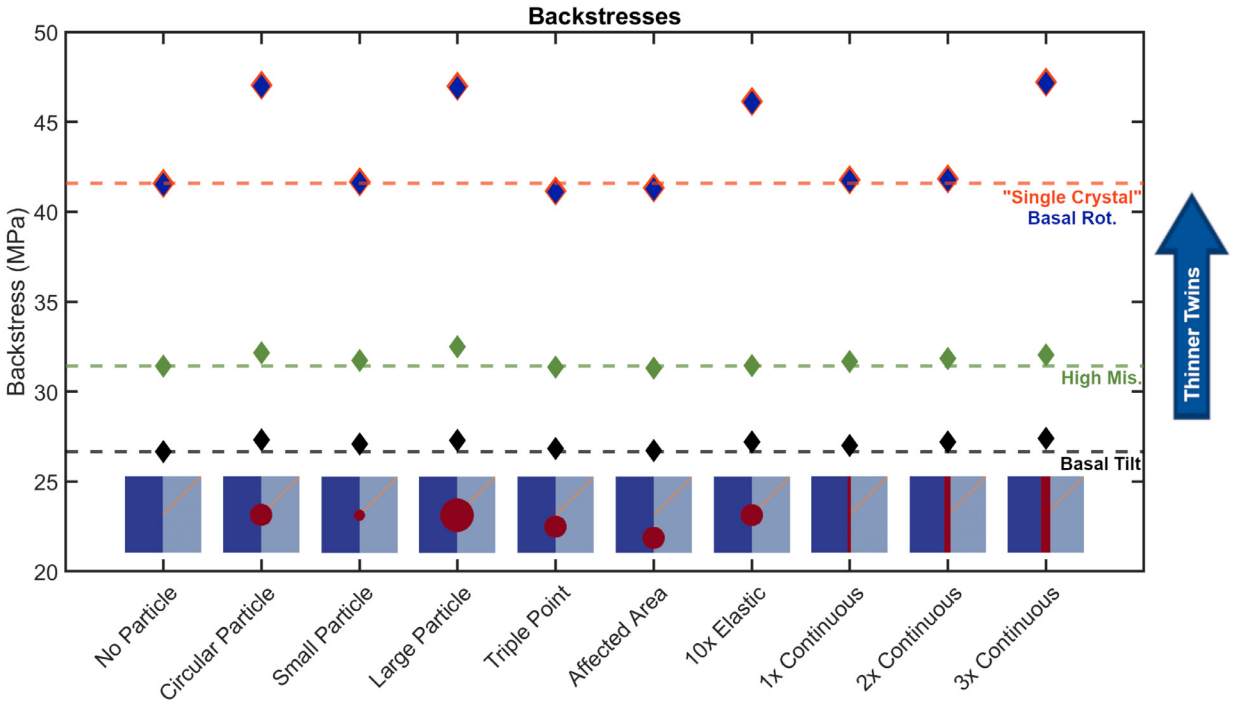

Fig. 6. Average backstress values of Σ regions for all cases, with dashed lines denoting the value for the case of no particle in the respective orientation. One standard deviation of error was calculated and found to fall within the height of the marker for all cases.

ing present, a decrease relative to a particle of equal size with a lower elastic modulus as seen in the circular particle case. Finally, unlike in the "single crystal" and basal rotation orientations, the continuous boundaries for these two orientations have a linear increase in backstress with boundary thickness.

3.4. Twin variants

The twin variant with the highest TRSS value is also calculated, as visualized in Fig. 7a-d. In these cases, only voxels with a TRSS above the critical resolved shear stress for twinning are denoted with the twin variant most likely to be active based on the resolved stress. For initial analysis into the effects of particles on twin variant selection, only the "single crystal" and basal rotation orientations were considered, as their resolved stresses are nearly identical. The variant selection was compared between the no particle and affected area microstructures, as both cases feature the twin impinging purely on the grain boundary. This ensures any modification to the active variants due to the stress state generated by the particle, rather than due to direct blocking of the impingement site.

In the "single crystal", portions of the regions where twinning is active appear noisy due to two variants having approximately equal TRSS values for a total of four active variants, whereas the basal rotation cases only have two. With the addition of the particle near the impingement site, new regions become active for twinning above the twin tip, and the shape of the separation between the regions of preferred variants is modified. Additionally, the changes to the active twin variant extend to the complete opposite side of the grain.

To better compare the modifications to the variant selection, the histograms in Fig. 7e and f show the number of voxels above the CRSS for twinning for each twin variant within an Ω region with a radius of 50 voxels around the twin tip, with the parent twin being variant 5. For a "single crystal" orientation with no par-

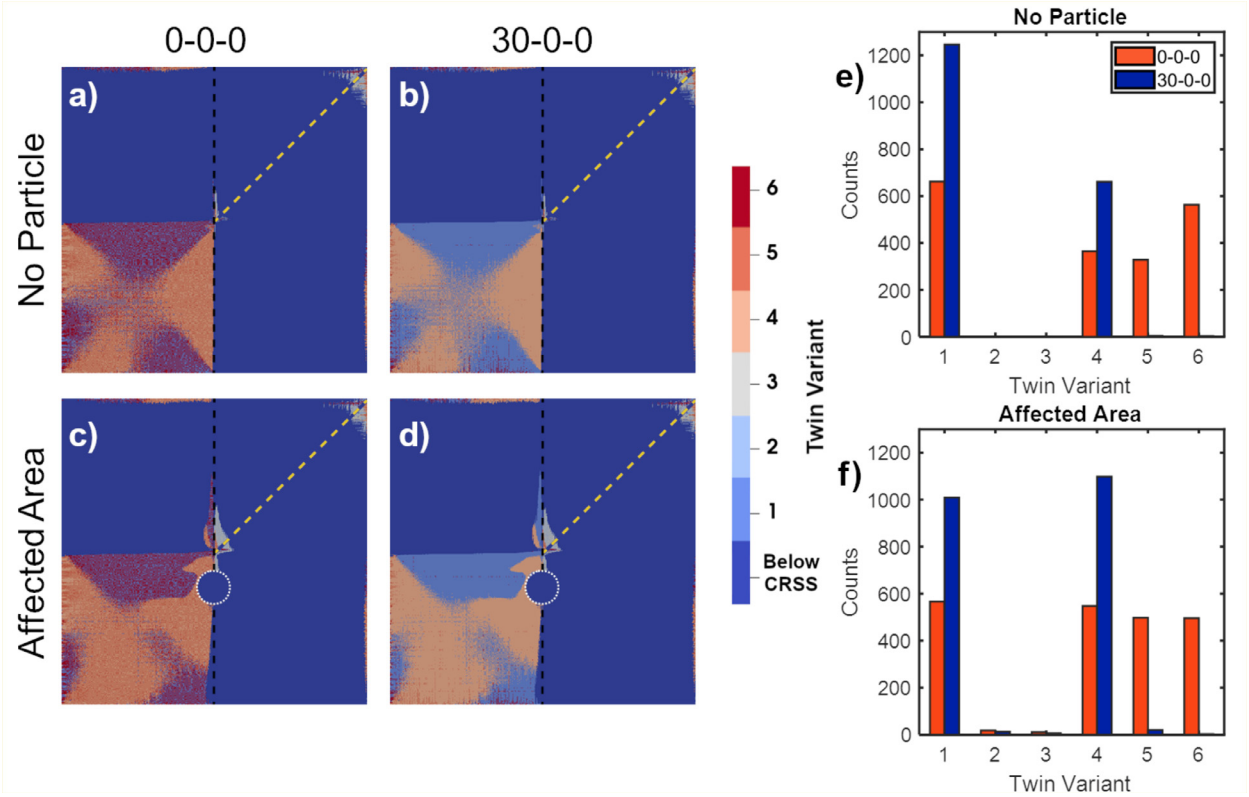

Fig. 7. Active twin variants during impingement near an intermetallic particle, determined by the variant with the highest TRSS at a given voxel. *a-d*) Visualizations of the active twin variants in voxels where the TRSS exceeds the CRSS for twinning. A schematic view (dashed lines) is overlaid to show the grain boundary (black), parent twin (yellow) and particle (white). *e-f*) Histograms of the number of voxels in which each variant is active within the Ω region (r=50) within the secondary grain. (For interpretation of the references to color in this figure legend, the reader is referred to the web version of this article.)

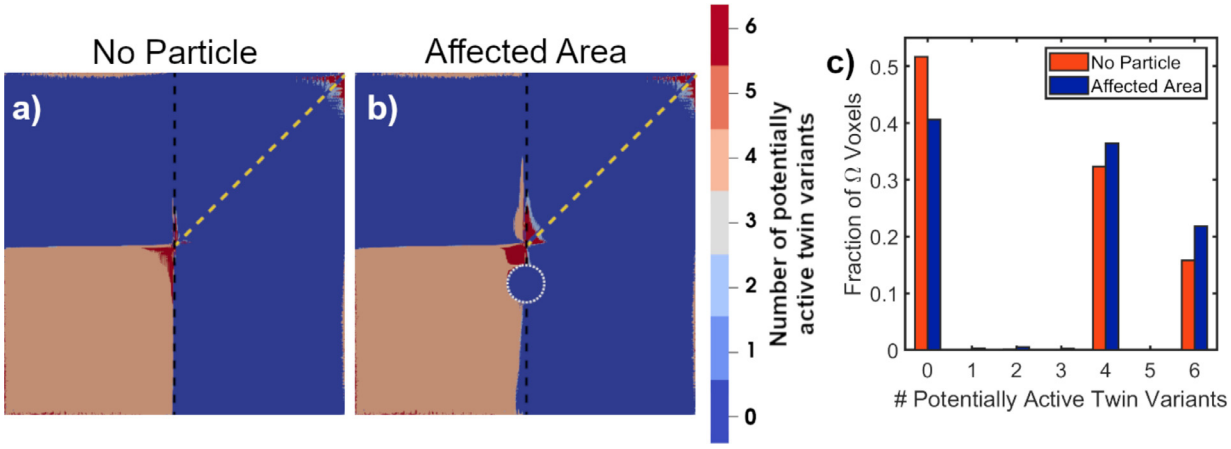

Fig. 8. Number of potentially active twin variants per voxel in the "single crystal" orientation, determined by the number of variants with resolved shear stresses greater than the CRSS for twinning. Visualizations of the *a*) no particle and *b*) affected area cases are shown with the same schematic view used in Fig. 7. *c*) Histogram of the fraction of voxels within the Ω region (r=50) for the given number of potentially active variants. The Basal Rotation (30-0-0) orientation was found to have similar results.

ticle, the stress states at each point result in variants 1 and 6 being approximately equal in activity, with 4 and 5 also being active to a lesser extent. However, with the addition of the intermetallic phase near the impingement site, variants 4 and 5 become more active to the point of matching the activity of 1 and 6. For basal rotation, variant 1 is strongly preferred with variant 4 approximately half as active within the Ω region when no particle is present. Once the particle is added in, however, the number of voxels where variant 1 is active decreases and variant 4's activity strongly increases, resulting in a slightly higher number of counts for variant 4 overall.

In addition to the most likely twin variant, the number of potentially active twin variants can also be considered, as seen in Fig. 8. The average TRSS values within the Ω region can be determined for each independent variant. The number of variants with a TRSS value greater than the CRSS for twinning can then be determined at any given voxel. This can be seen in Fig. 8a and b, where the addition of the particle near the impingement site in the "single crystal" orientation increases the amount of area near the twin tip where all six variants are potentially active. As before, an Ω region with a radius of 50 voxels is considered, and the fraction of voxels within the Ω for each number of potentially active

variants is shown in Fig. 8c. With the addition of the particle near the impingement site, more of the area within the Ω region has a stress state conducive to twinning, particularly with an increase in the amount of area where four and six of the twin variants are potentially active.

4. Discussion

The presence, size, mechanical properties, and relative position of coarse particles alter the stress state in the secondary grain, affecting both twin transmission and thickening. By considering these various morphological aspects, we can determine microstructural characteristics that are expected to lead to changes in the twinning behavior that lowers the frequency of twin transmission.

4.1. "Single crystal" and basal rotation orientations

The "single crystal" and basal rotation orientations have similar twinning resolved shear stress values and ratios due to the crystal symmetry aspect of the purely rotational difference between them, and thus are considered together. The addition of a coarse particle directly in the path of impingement sufficiently reduces the TRSS below the CRSS for twinning, preventing the twin transmission expected when no particle is present. However, the particle size appears to play an important role in the effectiveness, as decreasing the size led to an increase in the TRSS while further increasing the size had little additional effect. This indicates a critical particle size for the given grain boundary, below which particles only provide marginal benefits to preventing twin transmission whereas particles above this critical size are not expected to lead to a further reduction in the TRSS. For a real material, knowing this critical particle size would allow for optimized microstructural engineering, *e.g.*, heat treatments to be performed to optimally balance the volume fraction of the secondary phase in grain boundary particles and precipitates within the matrix.

Magnesium is prone to rapid fiber texture formation, aligning the basal poles during deformation and resulting in a microstructure full of 30° boundaries rotated around the $\langle c \rangle$-axis [31,32]. This deformation texture remains and strengthens during heat treatments, with necklace recrystallization leading to the nucleated grains only rotating relative to the parent [1,33,34]. The grain boundaries seen in deformed magnesium, even after recrystallization, primarily fall within the range bounded by the "single crystal" and basal rotation orientations. Finding the critical particle size for reducing the TRSS is most important in these grain orientations for reducing transmission in wrought products.

The elastic modulus may play a role in determining this critical size as increasing the modulus without modifying the particle morphology similarly decreased the ability of the particle to prevent twin transmission, likely due to the inability of the particle to elastically deform to help accommodate shear from the parent twin. In this instance, an elastically harder intermetallic may need to be larger to reach the critical size, while an elastically softer phase would be more effective even at smaller diameters. The Young's modulus for β-$Mg_{17}Al_{12}$ is approximately 80 GPa, making Mg_2Ca comparatively softer at 44.1 GPa [35]. Magnesium-strontium alloys also offer elastically softer intermetallic phases, with Mg_2Sr and $Mg_{17}Sr_2$ having a Young's modulus of 34.3 and 50.6 GPa respectively, [36] while Mg_2Pb is slightly closer to the β-phase at 66.7 GPa [37]. This range of elastic hardness in intermetallic phases makes alloy chemistry and the specific phase formed an important factor in determining the critical particle size for preventing twin transmission.

Another scenario that must be considered is instances in which the particle is softer than the matrix. While this is unlikely to occur in magnesium alloys as primarily considered here, the possibility exists within the realm of titanium alloys. In near-α two-phase Ti alloys, it is possible to form deformation twins within the hexagonal closed packed α phase [38]. In two-phase Ti, localized regions of body centered cubic β phase may be present between α grain boundaries, creating the possibility for a twin to impinge on what is effectively a softer particle [39]. In this instance, both the elastic constants as well as the plastic behavior of the β titanium would need to be taken into account within the model, but the resultant stress in the neighboring α grain and the likelihood of twin transmission could be examined. While some aspects of the deformation behavior such as slip transmission between the phases would be lost, this could prove to be a useful method for simulating this interaction in Ti; however, further computational work and experimental validation would be needed.

In addition to particle size, particle spacing must also be considered when preventing twin transmission as seen in the "near misses" of the triple point and affected area cases, where the twin does not impinge directly on the bulk of the particle. In these instances, having a particle close to the impingement site increases the chances of nucleating a secondary twin, making their presence detrimental. As the associated stresses were found to be higher when the twin tip was in the area near the particle rather than directly hitting the triple point, this poses a balancing act for microstructural control. For a given particle volume fraction in a bulk material, larger particles that are spaced further apart may not prove to be as effective at preventing twin transmission as smaller particles that are closer together, even though the individual particles for the latter case do not reduce the TRSS to the same degree. This is similar to the considerations already used in microstructural engineering for other aspects such as controlling grain size via Zener pinning. Heat treatments above the β solvus will decrease the grain boundary particle size and increase the spacing, allowing for control over both of these factors [40].

One way to balance the sizing and spacing of these particles is to consider the aspect ratio, as in the continuous boundary cases that are representative of the as-solidified state of cast Mg-Al alloys [22,23]. While the thickest boundary was found to reduce the TRSS in the neighboring grain, a highly continuous network of the β phase along the grain boundaries have been shown to greatly reduce ductility, contributing to brittle failure [2]. It should be noted that the 3× continuous boundary case has a thickness of 21 voxels, which is thinner than the diameter of the small particle (D = 25) yet the boundary results in a larger overall decrease in the TRSS except for at very short range. Aspect ratio is then a key factor in determining the efficacy of a particle at preventing twin transmission rather than size alone.

While the majority of research on twinning in multi-phase magnesium alloys has focused on sub-micron precipitates, some observations have been made in systems containing micron-scale intermetallic particles. Patel et al. [41,42] examined the microstructure of several thixomolded AZ91D and AM60B subjected to tensile loading and fatigue, where they observed a number of twins within the microstructure that are arrested by the coarse intermetallic network at the grain boundaries. Conversely, in another of Patel's works on cyclic loading of AZ91D [43], there appears to be a set of twins that reflect the "near misses" of the triple point and affected area microstructures in which both result in apparent transmission into the neighboring grains; however, orientation information for the grains would be needed to determine whether transmission would be expected in this instance without the presence of the particles. It is also notable that the boundaries of the twinned regions within these experiments appear to deflect along their length rather than forming the parallel bands or classic lenticular shape, as is usually seen during cyclic loading of Mg alloys without these intermetallic particles [44,45]. This may be due to the stress states induced within the grain by in-

teractions with coarse particles outside of the plane being viewed, but three-dimensional datasets would be needed for more explicit determination.

Orozco-Caballero et al. [46] captured the interaction between a twin and an intragranular β-phase particle in AZ31 while using high-resolution digital image correlation (HRDIC), resulting in an example similar to the small particle "single crystal" case. In this instance, the twin was observed to have grown to entirely engulf the β-phase region, with the HRDIC revealing a localized region of strain at the edge of the particle. Asgari et al. [47] studied the effects of yttrium content in AE alloys under shock loading conditions, with an increase from 2 to 4% Y resulting in an increased fraction of the Al_2Y intermetallic phase and a subsequent decrease in twinning activity. However, the increased yttrium content was also associated with an increase in dislocation density and thus slip activity, making it unclear how much of the reduction in twinning is directly associated with the presence of more particles. Similarly, Park et al. [48] found that the addition of artificial cooling to high speed extrusion of Mg-7Sn-1Al-1Zn both increased the number of Mg_2Sn particles present in the material and decreased the twin volume fraction after tensile deformation. The degree to which these particles can be directly attributed to reducing twinning is once again difficult to determine as this artificial cooling also resulted in a reduction in grain size, which is associated with a reduction in twin area [10]. Further experimental studies would be needed to deconvolve the reduction in twinning due solely to the presence of particles from that of alloy composition or grain size.

4.2. High misorientation

In the highly misoriented grains, many of the trends observed in the other orientations considered no longer hold. The addition of any particle increases the resultant TRSS compared to when no particle is present, making all instances of particles at or near the twin impingement site more likely to result in transmission across the grain boundary. The elastic response of the intermetallic phase likely imparts a stress on the neighboring grain in a direction that remains favorable for twinning, resulting in the small particle to have a lower TRSS than either the circular or large particle cases. Increasing the elastic modulus in this orientation results in a short-range decrease in the stress.

For this crystal orientation, the twin tip meeting the triple point at the particle edge only has a high stress very locally to the impingement site, at which point compressive stresses appear to counteract some of the elements of the stress state, resulting in a lower TRSS than when the particle lies directly in the twin's path. Moving the particle further away seems to remove this effect, increasing with Ω radius whereas the triple point case decreases. Due to this shift, twin transmission into the secondary grain may occur locally to the triple point, but a particle further away may result in a twin nucleating elsewhere along the boundary instead. Prior studies on twin transmission have focused on instances of twins in contact across a grain boundary, such as adjoined twin pairs or twin chains [10,12,15]. These methods would not account for transmission events caused by the presence of a nearby coarse particle, potentially leading to under-reporting of this phenomenon in material with grain boundary particles.

This orientation case deviates from the rest in that increasing the thickness of the continuous boundaries does not induce a significant decrease in TRSS. As in other instances, the elastic response of the intermetallic phase likely imparts a stress on the neighboring grain in a direction that remains favorable for twinning. Since there is a slight increase in stress between the thinnest boundary and the two thicker boundaries, further increase in this continuous β layer thickness may not lower the stress in the secondary grain. These instances are the most likely source of twin transmission between grains for this orientation case. This complicates the design of an idealized microstructure for preventing twin transmission, as the particle size and aspect ratio that works best for highly textured sheet may make transmission more frequent in a randomly oriented sheet. However, it is important to note that this behavior may not be true for all grains with this amount of misorientation, as this may be a portion of orientation space that results in being particularly favorable for twinning in this instance. Further study into additional crystal orientations may be warranted to more thoroughly determine these relations.

4.3. Twin thickening

The backstresses seen here indicate a reversal in the twin shear stress across the entirety of the twinned region, in agreement with what has been observed experimentally at the onset of twinning [49]. While it is generally pertinent to consider the twin aspect ratio when discussing twin thickening as the backstress is a function of the twin thickness, Kumar et al. reported qualitatively similar results when the twin volume fraction, which is related to the aspect ratio, was changed [13,18]. For this reason, only a single twin aspect ratio was used to ensure the twin was small relative to the size of the boundary particle. Due to this aspect ratio, the observed trends in backstresses are limited to the thin twins typical for the onset of twinning, with aspect ratios on the order of 1/50. As the twin thickness increases, the additional localized plasticity may lead to a breakdown in these trends so the observations made here may no longer hold.

Comparing across the various cases, the orientation of the neighbor serves as the primary determining factor in the backstress generated within the parent grain during the twinning shear transformation. While secondary, the local microstructure also appears to play a role in determining the final twin thickness. Particularly in the orientations more favorably aligned for twin transmission, the cases in which there is a direct obstacle of sufficient thickness experience an increased backstress, leading to thinner twins. As these are also the cases in which twin transmission is least expected to occur, the combination of these effects would likely result in a noticeably diminished twin volume fraction.

In the instances where twin transmission is expected to be unaffected or even made to be more likely, there is little observed decrease in the resultant backstress, and thus these cases are not expected to undergo significant twin growth beyond that seen in grain boundary devoid of intermetallic. However, computational studies have shown that after twin nucleation in the neighboring grain backstress within the parent grain dramatically decrease, allowing thickening near the impingement site [19]. Evidence of this has also been seen experimentally, where twins conjoined at grain boundaries were found to have a higher average thickness than either independent counterparts [10]. Thus, while these cases may not inherently lead to thicker twins in instances where twin transmission does not occur, any resulting nucleation of a twin in the secondary grain would ultimately lead to further twin thickening.

4.4. Twin variant selection

The addition of a grain boundary particle near the twin tip, even when not directly in the path of the parent twin, is found to modify the relative activities of the twin variants. This is especially notable as there is little change in twinning resolved shear stress between the two crystal orientations, yet basal rotation undergoes a more prominent increase of a particular variant. The presence of a particle near the twin modifies the variant selection, shifting it away from what would be expected under normal conditions. Non-Schmid twin variant selection has long been observed

in HCP materials, but the reasons for this phenomenon have been unclear [10,50–53]. The present results suggest that intermetallic grain boundary particles may partially account for the observed non-Schmid behavior, and may warrant further study.

Similarly, the addition of a particle near the twin tip was seen to increase the number of twin variants that are potentially active within the region immediately adjacent to the impingement site. As twinning nucleation is a statistical event requiring both a favorable defect structure and a favorable stress state [54–56], increasing the number of potentially active variants is expected to subsequently increase the frequency of twin transmission. However, this would also increase the likelihood of the resultant twin being a different variant than the parent, even when crossing into a grain with a nearly identical orientation. This could result in the nucleation of twin variants that are less favorable for propagation through the neighboring grain and the potential termination of the twin chain, and may be an aspect of twin transmission that also warrants further experimental study.

5. Conclusions

Crystal Plasticity – Fast Fourier Transform modeling has been used to determine how coarse intermetallic particles that form at grain boundaries affect twinning behavior in both the parent and neighboring grains by modifying the local stress states. The results of the model suggest the following:

- Particles directly in the path of twin impingement lowered the TRSS in the neighboring grain, reducing the likelihood of twin transmission across the boundary.
- Grain boundary misorientation had a larger effect on the TRSS than particle presence, but particles can alter behavior in important cases such as basal rotation.
- Increasing particle size decreased the TRSS until a critical size was reached, above which further increases did not continue to modify the stress in the neighboring grain.
- The critical particle size appeared to be dependent upon the combination of particle aspect ratio, elastic modulus of the intermetallic phase, and the orientation of the grains.
- Twins impinging near or immediately adjacent to a particle had an increased likelihood of transmission.
- Microstructures expected to reduce the likelihood of twin transmission also experienced a higher backstress, which would lead to thinner twins. Cases that were more likely to transmit a twin did not have a significantly lowered backstress.
- The inclusion of a particle near the impingement site modified the relative activity of twin variants present in the neighboring grain, which may help to explain widely observed non-Schmid twin variant selection.

Declaration of Competing Interest

The authors declare that they have no known competing financial interests or personal relationships that could have appeared to influence the work reported in this paper.

Acknowledgement

Authors B.A. and B.L. were supported by the National Defense Science & Engineering Graduate Fellowship. We acknowledge the computing resources provided on Henry2, a high-performance computing cluster operated by North Carolina State University. I.J.B. acknowledges financial support from the National Science Foundation Designing Materials to Revolutionize and Engineer our Future (DMREF) program (NSF CMMI-1729887).

Supplementary material

The stress data files and analysis scripts used in this work are available online at https://github.com/MONSTERgroup/CPFFT_Def_Twin_Analysis for the purposes of data visualization and further analysis. Additional data files produced by the simulations will be made available upon reasonable request.

Supplementary material associated with this article can be found, in the online version, at doi:10.1016/j.actamat.2021.117225.

References

[1] J.F. Nie, K.S. Shin, Z.R. Zeng, Microstructure, Deformation, and Property of Wrought Magnesium Alloys, Springer US, 2020, doi:10.1007/s11661-020-05974-z.
[2] A.A. Luo, P. Fu, L. Peng, X. Kang, Z. Li, T. Zhu, Solidification microstructure and mechanical properties of cast magnesium-aluminum-tin alloys, Metall. Mater. Trans. A 43 (1) (2012) 360–368, doi:10.1007/s11661-011-0820-y.
[3] T.D. Berman, T.M. Pollock, J.W. Jones, Texture, second-phase particles, and the anisotropy of deformation behavior in TTMP AZ61, Metall. Mater. Trans. A 46 (7) (2015) 2986–2998, doi:10.1007/s11661-015-2913-5.
[4] J.D. Robson, N. Stanford, M.R. Barnett, Effect of precipitate shape and habit on mechanical asymmetry in magnesium alloys, Metall. Mater. Trans. A 44 (7) (2013) 2984–2995, doi:10.1007/s11661-012-1466-0.
[5] N. Stanford, M.R. Barnett, Effect of particles on the formation of deformation twins in a magnesium-based alloy, Mater. Sci. Eng. A 516 (1–2) (2009) 226–234, doi:10.1016/j.msea.2009.04.001.
[6] D. Ando, J. Koike, Y. Sutou, The role of deformation twinning in the fracture behavior and mechanism of basal textured magnesium alloys, Mater. Sci. Eng. A 600 (2014) 145–152, doi:10.1016/j.msea.2014.02.010.
[7] D.W. Brown, S.R. Agnew, M.A.M. Bourke, T.M. Holden, S.C. Vogel, C.N. Tomé, Internal strain and texture evolution during deformation twinning in magnesium, Mater. Sci. Eng. A 399 (1–2) (2005) 1–12, doi:10.1016/j.msea.2005.02.016.
[8] D. Ando, J. Koike, Y. Sutou, Relationship between deformation twinning and surface step formation in AZ31 magnesium alloys, Acta Mater. 58 (13) (2010) 4316–4324, doi:10.1016/j.actamat.2010.03.044.
[9] D.A. Basha, H. Somekawa, A. Singh, Crack propagation along grain boundaries and twins in Mg and Mg-0.3 at.%Y alloy during in-situ straining in transmission electron microscope, Scr. Mater. 142 (2018) 50–54, doi:10.1016/j.scriptamat.2017.08.023.
[10] I.J. Beyerlein, L. Capolungo, P.E. Marshall, R.J. McCabe, C.N. Tome, Statistical analyses of deformation twinning in magnesium, Philos. Mag. 90 (16) (2010) 2161–2190, doi:10.1080/14786431003630835.
[11] A. Ghaderi, M.R. Barnett, Sensitivity of deformation twinning to grain size in titanium and magnesium, Acta Mater. 59 (20) (2011) 7824–7839, doi:10.1016/j.actamat.2011.09.018.
[12] B. Wang, J. Shi, P. Ye, L. Deng, N. Guo, C. Wang, J. Chen, Q. Li, Analysis of {10-12} twinning variants' selection behavior during multi-directional compression in Mg-3Al-1Zn magnesium alloy, Journal of Materials Science 54 (13) (2019) 9797–9808, doi:10.1007/s10853-019-03561-1.
[13] M. Arul Kumar, A.K. Kanjarla, S.R. Niezgoda, R.A. Lebensohn, C.N. Tomé, Numerical study of the stress state of a deformation twin in magnesium, Acta Mater. 84 (2015) 349–358, doi:10.1016/j.actamat.2014.10.048.
[14] M. Arul Kumar, I.J. Beyerlein, R.J. McCabe, C.N. Tomé, Grain neighbour effects on twin transmission in hexagonal close-packed materials, Nat. Commun. 7 (May) (2016) 1–9, doi:10.1038/ncomms13826.
[15] G. Liu, R. Xin, F. Liu, Q. Liu, Twinning characteristic in tension of magnesium alloys and its effect on mechanical properties, Mater. Des. 107 (2016) 503–510, doi:10.1016/j.matdes.2016.06.073.
[16] M. Arul Kumar, I.J. Beyerlein, C.N. Tomé, Grain size constraints on twin expansion in hexagonal close packed crystals, J. Appl. Phys. 120 (15) (2016), doi:10.1063/1.4965719.
[17] I.J. Beyerlein, X. Zhang, A. Misra, Growth twins and deformation twins in metals, Annual Review of Materials Research 44 (2014) 329–363, doi:10.1146/annurev-matsci-070813-113304.
[18] M. Arul Kumar, I.J. Beyerlein, C.N. Tomé, Effect of local stress fields on twin characteristics in HCP metals, Acta Mater. 116 (2016) 143–154, doi:10.1016/j.actamat.2016.06.042.
[19] M. Arul Kumar, L. Capolungo, R.J. McCabe, C.N. Tomé, Characterizing the role of adjoining twins at grain boundaries in hexagonal close packed materials, Sci. Rep. 9 (1) (2019) 3846, doi:10.1038/s41598-019-40615-5.
[20] M. Arul Kumar, I.J. Beyerlein, R.A. Lebensohn, C.N. Tomé, Role of alloying elements on twin growth and twin transmission in magnesium alloys, Mater. Sci. Eng. A 706 (August) (2017) 295–303, doi:10.1016/j.msea.2017.08.084.
[21] M. Arul Kumar, I.J. Beyerlein, C.N. Tomé, A measure of plastic anisotropy for hexagonal close packed metals: application to alloying effects on the formability of Mg, J. Alloys Compd. 695 (2017) 1488–1497, doi:10.1016/j.jallcom.2016.10.287.
[22] A.K. Dahle, Y.C. Lee, M.D. Nave, P.L. Schaffer, D.H. StJohn, Development of the as-cast microstructure in magnesium-aluminium alloys, J. Light Metals 1 (1) (2001) 61–72, doi:10.1016/S1471-5317(00)00007-9.

[23] B. Kondori, R. Mahmudi, Effect of Ca additions on the microstructure, thermal stability and mechanical properties of a cast AM60 magnesium alloy, Mater. Sci. Eng. A 527 (7–8) (2010) 2014–2021, doi:10.1016/j.msea.2009.11.043.
[24] M.S. Dargusch, K. Pettersen, K. Nogita, M.D. Nave, G.L. Dunlop, The effect of aluminium content on the mechanical properties and microstructure of die cast binary magnesium-aluminium alloys, Mater. Trans. 47 (4) (2006) 977–982, doi:10.2320/matertrans.47.977.
[25] R. Decker, S. Lebeau, T. Berman, T. Miller, J.W. Jones, T. Pollock, N. Moskovich, B. Bronfin, Thermomechanical processing of thixomolded alloys, in: Magnesium Technology, 2017, pp. 235–243, doi:10.1007/978-3-319-52392-7.
[26] Z.W. Huang, Y.H. Zhao, H. Hou, P.D. Han, Electronic structural, elastic properties and thermodynamics of Mg17Al12, Mg2Si and Al2Y phases from first-principles calculations, Physica B 407 (7) (2012) 1075–1081, doi:10.1016/j.physb.2011.12.132.
[27] I.J. Beyerlein, R.J. McCabe, C.N. Tomé, Effect of microstructure on the nucleation of deformation twins in polycrystalline high-purity magnesium: a multi-scale modeling study, J. Mech. Phys. Solids 59 (5) (2011) 988–1003, doi:10.1016/j.jmps.2011.02.007.
[28] K. Hagihara, K. Hayakawa, Plastic deformation behavior and operative slip systems in Mg17Al12 single crystals, Mater. Sci. Eng. A 737 (September) (2018) 393–400, doi:10.1016/j.msea.2018.09.056.
[29] S.W. Xu, N. Matsumoto, S. Kamado, T. Honma, Y. Kojima, Effect of Mg17Al12 precipitates on the microstructural changes and mechanical properties of hot compressed AZ91 magnesium alloy, Mater. Sci. Eng. A 523 (1–2) (2009) 47–52, doi:10.1016/j.msea.2009.05.032.
[30] V.M. Miller, T.M. Pollock, Texture modification in a magnesium-aluminum-calcium alloy during uniaxial compression, Metall. Mater. Trans. A 47 (4) (2016) 1854–1864, doi:10.1007/s11661-016-3351-8.
[31] S.R. Agnew, M.H. Yoo, C.N. Tomé, Application of texture simulation to understanding mechanical behavior of Mg and solid solution alloys containing Li or Y, Acta Mater. 49 (20) (2001) 4277–4289, doi:10.1016/S1359-6454(01)00297-X.
[32] J.J. Bhattacharyya, S.R. Agnew, G. Muralidharan, Texture enhancement during grain growth of magnesium alloy AZ31B, Acta Mater. 86 (2015) 80–94, doi:10.1016/j.actamat.2014.12.009.
[33] M.R. Barnett, A. Sullivan, N. Stanford, N. Ross, A. Beer, Texture selection mechanisms in uniaxially extruded magnesium alloys, Scr. Mater. 63 (7) (2010) 721–724, doi:10.1016/j.scriptamat.2010.01.018.
[34] R.K. Nadella, I. Samajdar, G. Gottstein, Static recrystallisation and textural changes in warm rolled pure magnesium, Magnesium (2005) 1052–1057, doi:10.1002/3527603565.ch163.
[35] Z. Yang, J. Du, B. Wen, C. Hu, R. Melnik, First principles studies on the structural, elastic, electronic properties and heats of formation of Mg-AE (AE = Ca, Sr, Ba) intermetallics, Intermetallics 32 (2013) 156–161, doi:10.1016/j.intermet.2012.09.002.
[36] D. Zhou, J. Liu, S. Xu, P. Peng, First-principles investigation of the binary intermetallics in Mg-Al-Sr alloy: stability, elastic properties and electronic structure, Comput. Mater. Sci. 86 (2014) 24–29, doi:10.1016/j.commatsci.2014.01.007.
[37] Y.H. Duan, Y. Sun, J. Feng, M.J. Peng, Thermal stability and elastic properties of intermetallics Mg2Pb, Physica B 405 (2) (2010) 701–704, doi:10.1016/j.physb.2009.09.090.
[38] Y. Yu, R. Chen, C.L. Li, W. Ye, S. Hui, A study on microstructural evolution and detwinning behavior of Ti-3Al-2.5V cold-rolled tube during annealing, Mater. Res. Express 7 (9) (2020), doi:10.1088/2053-1591/abba4f.
[39] D. Banerjee, J.C. Williams, Perspectives on titanium science and technology, Acta Mater. 61 (3) (2013) 844–879, doi:10.1016/j.actamat.2012.10.043.
[40] T. Zhu, Z.W. Chen, W. Gao, Dissolution of eutectic β-Mg 17Al 12 phase in magnesium Az91 cast alloy at temperatures close to eutectic temperature, J. Mater. Eng. Perform. 19 (6) (2010) 860–867, doi:10.1007/s11665-009-9539-y.
[41] H.A. Patel, D.L. Chen, S.D. Bhole, K. Sadayappan, Microstructure and tensile properties of thixomolded magnesium alloys, J. Alloys Compd. 496 (1–2) (2010) 140–148, doi:10.1016/j.jallcom.2010.02.042.
[42] H.A. Patel, D.L. Chen, S.D. Bhole, K. Sadayappan, Low cycle fatigue behavior of a semi-solid processed AM60B magnesium alloy, Mater. Des. 49 (2013) 456–464, doi:10.1016/j.matdes.2013.01.015.
[43] H.A. Patel, D.L. Chen, S.D. Bhole, K. Sadayappan, Cyclic deformation and twinning in a semi-solid processed AZ91D magnesium alloy, Mater. Sci. Eng. A 528 (1) (2010) 208–219, doi:10.1016/j.msea.2010.09.016.
[44] C.F. Gu, L.S. Toth, M. Hoffman, Twinning effects in a polycrystalline magnesium alloy under cyclic deformation, Acta Mater. 62 (1) (2014) 212–224, doi:10.1016/j.actamat.2013.09.048.
[45] S. Dong, Q. Yu, Y. Jiang, J. Dong, F. Wang, W. Ding, Electron backscatter diffraction observations of twinning-detwinning evolution in a magnesium alloy subjected to large strain amplitude cyclic loading, Mater. Des. 65 (2015) 762–765, doi:10.1016/j.matdes.2014.09.079.
[46] A. Orozco-Caballero, D. Lunt, J.D. Robson, J. Quinta da Fonseca, How magnesium accommodates local deformation incompatibility: a high-resolution digital image correlation study, Acta Mater. 133 (2017) 367–379, doi:10.1016/j.actamat.2017.05.040.
[47] H. Asgari, A.G. Odeshi, J.A. Szpunar, L.J. Zeng, E. Olsson, D.Y. Li, Effect of yttrium on the twinning and plastic deformation of AE magnesium alloy under ballistic impact, Mater. Sci. Eng. A 623 (2015) 10–21, doi:10.1016/j.msea.2014.11.025.
[48] S.H. Park, S.H. Kim, H.S. Kim, B.S. You, Improved strength of Mg alloy extruded at high speed with artificial cooling, J. Alloys Compd. 648 (2015) 615–621, doi:10.1016/j.jallcom.2015.06.219.
[49] M. Barnett, M. Setty, F. Siska, Estimating critical stresses required for twin growth in a magnesium alloy, Metall. Mater. Trans. A 44 (7) (2013) 2962–2969, doi:10.1007/s11661-012-1573-y.
[50] M.R. Barnett, Z. Keshavarz, A.G. Beer, X. Ma, Non-Schmid behaviour during secondary twinning in a polycrystalline magnesium alloy, Acta Mater. 56 (1) (2008) 5–15, doi:10.1016/j.actamat.2007.08.034.
[51] A. Jain, O. Duygulu, D.W. Brown, C.N. Tomé, S.R. Agnew, Grain size effects on the tensile properties and deformation mechanisms of a magnesium alloy, AZ31B, sheet, Mater. Sci. Eng. A 486 (1–2) (2008) 545–555, doi:10.1016/j.msea.2007.09.069.
[52] M.R. Barnett, Z. Keshavarz, M.D. Nave, Microstructural features of rolled Mg-3Al-1Zn, Metall. Mater. Trans. A 36 (7) (2005) 1697–1704, doi:10.1007/s11661-005-0033-3.
[53] Z.Z. Shi, Y. Zhang, F. Wagner, P.A. Juan, S. Berbenni, L. Capolungo, J.S. Lecomte, T. Richeton, On the selection of extension twin variants with low Schmid factors in a deformed Mg alloy, Acta Mater. 83 (2015) 17–28, doi:10.1016/j.actamat.2014.10.004.
[54] J. Wang, I.J. Beyerlein, C.N. Tomé, An atomic and probabilistic perspective on twin nucleation in Mg, Scr. Mater. 63 (7) (2010) 741–746, doi:10.1016/j.scriptamat.2010.01.047.
[55] S.R. Niezgoda, A.K. Kanjarla, I.J. Beyerlein, C.N. Tomé, Stochastic modeling of twin nucleation in polycrystals: An application in hexagonal close-packed metals, Int. J. Plast. 56 (2014) 119–138, doi:10.1016/j.ijplas.2013.11.005.
[56] I.J. Beyerlein, C.N. Tomé, A probabilistic twin nucleation model for HCP polycrystalline metals, Proc. R. Soc. A 466 (2121) (2010) 2517–2544, doi:10.1098/rspa.2009.0661.